PNAS

Supporting Information for

Discontinuous instabilities in disordered solids

Ding Xu, Shiyun Zhang, Andrea J. Liu, Sidney R. Nagel, Ning Xu

To whom correspondence should be addressed. E-mail: ningxu@ustc.edu.cn

This PDF file includes:

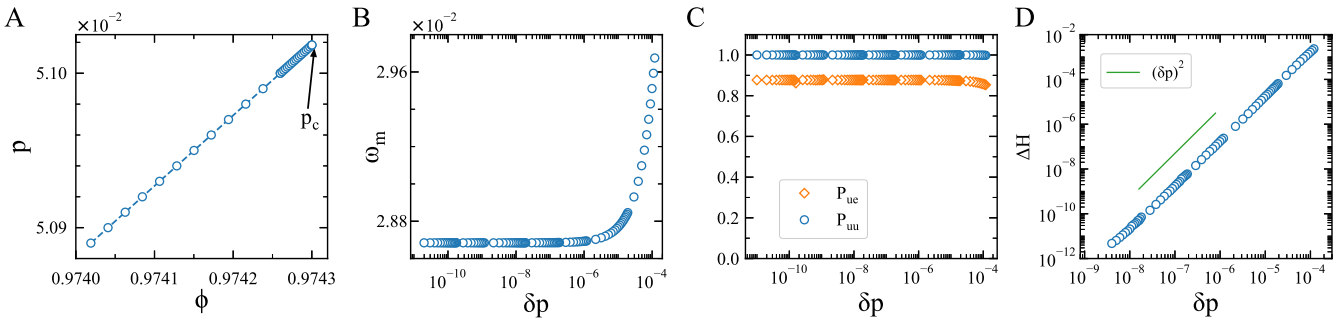

Fig. S1. An example of discontinuous instability under compression for a 2D jammed packing of $N = 1024$ particles interacting via the harmonic potential initially at $p = 5 \times 10^{-2}$. (A) The pressure, p, is shown versus packing fraction, ϕ, on approaching the instability at $p = p_c$. (B) The frequency of the lowest normal mode of vibration, ω_m, is shown versus the distance from the instability, $\delta p \equiv p_c - p$. (C) The projections of the particle displacements onto the lowest normal mode, P_{ue}, and the particle displacements right at the instability, P_{uu}, are shown versus δp. (D) The energy barrier height, ΔH, is shown versus δp.

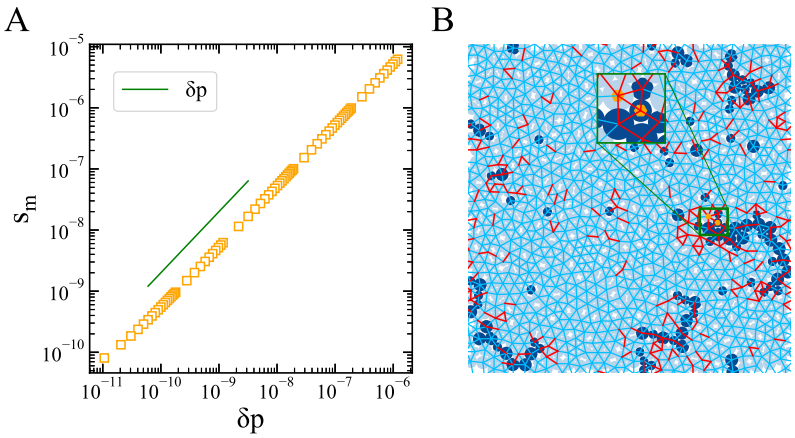

Fig. S2. Bond-breaking as the cause of the discontinuous instability for a jammed packing of $N = 1024$ particles interacting via the harmonic potential under compression. (A) Minimum particle overlap $s_m(\delta p)$ on approaching the instability. The solid line shows $s_m \sim \delta p$. (B) Configuration of the jammed packing near the instability with the force network. Stabilizing bonds are in red. The bond whose breaking leads to the instability at p_c is highlighted by the orange dots. Softest particles with top 10% Ψ values are highlighted in dark blue.

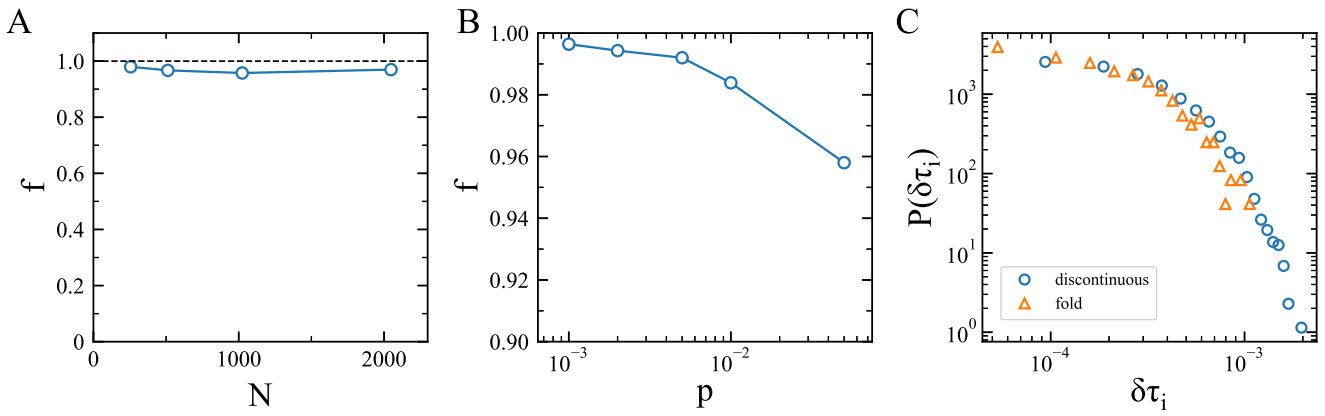

Fig. S3. Statistics of discontinuous instabilities. (A) Fraction of discontinuous instabilities f as a function of system size N for 2D jammed packings with the harmonic potential. It shows a very weak dependence on N. The discontinuous instabilities apparently far outnumbers the fold instabilities with $f > 0.95$ for all system sizes shown here. The solid line is a guide to the eye. The horizontal dashed line is $f = 1$. (B) Pressure evolution of the fraction of discontinuous instabilities f for $N = 1024$ harmonic systems in 2D. With the decrease of pressure, f increases and shows the trend to approach 1 in the low pressure limit. The solid line is a guide to the eye. (c) Distributions of shear stresses at incipient discontinuous and fold instabilities for $N = 1024$ harmonic systems initially at $p = 5 \times 10^{-2}$ in 2D. Here $\delta\tau_i = \tau_c - \tau_i$, where τ_c is the shear stress at the instability and τ_i is the residue shear stress of the initial state before shearing.

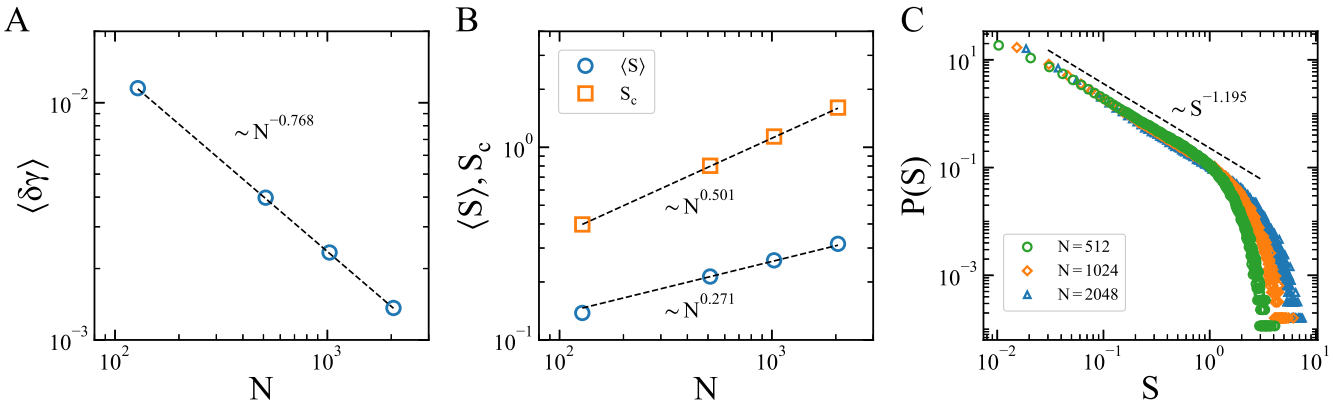

Fig. S4. Statistics of plastic events induced by discontinuous instabilities in steady, quasistatic shear flows. The systems contain N particles interacting via the harmonic repulsive potential in 2D and initially at $p = 5 \times 10^{-2}$. They are quasistatically sheared to steady state and then avalanches are studied. (A) System size dependence of the average strain interval between successive avalanches $\langle\delta\gamma\rangle$. (B) System size dependence of the mean and cutoff avalanche sizes, $\langle S\rangle$ and S_c. (C) System size evolution of the distribution of avalanche sizes $P(S)$. The dashed lines are power-law fittings to the data. The avalanche size is calculated as $S = L^d\Delta\sigma$, where L is the sidelength of the system, d is the spatial dimension (here $d = 2$), and $\Delta\sigma$ is the stress drop of the avalanche. The cutoff avalanche size is calculated as $S_c \equiv \langle S^2\rangle/\langle S\rangle$. Please refer to Ref. (1) for the definitions and calculations of the above quantities. It has been shown that there exist critical scaling relations, e.g., $\langle\delta\gamma\rangle \sim N^{-\chi}$, $\langle S\rangle \sim N^{\alpha}$, $S_c \sim L^{d_f} \sim N^{d_f/d}$, and $P(S) \sim S^{-\tau}$ (1). Here we have $\chi \approx 0.768$, $\alpha \approx 0.271$, $d_f \approx 1.002$, and $\tau \approx 1.195$. Recent theories predict different values of the critical exponents, e.g., $\chi = 1$ or 0.667, $\tau = 1.5$ or 1.0 (2–4). Our results show some deviations from theoretical predictions. Assuming the hyperscaling relation, $\tau = 2 - (1 - \chi)d/d_f$ (1), our values of χ and τ give a fractal dimension $d_f \approx 0.576$, only about a half of the d_f value obtained from (B). Interestingly, a similar violation of the hyperscaling relation has been observed in recent work on the two-scale percolation scenario of the jamming transition (5). The violation may be caused by the marginal stability of jammed solids due to the finite-range repulsive interaction at low packing fractions. Intensive studies are required to figure out whether discontinuous and fold instabilities have different avalanche statistics and what leads to the violation of the hyperscaling relation, which is beyond the scope of current work.

References

1. N. Oyama, H. Mizuno, and A. Ikeda, Unified view of avalanche criticality in sheared glasses, *Phys. Rev. E* **104**, 015002 (2021).
2. K. A. Dahmen, Y. Ben-Zion, and J. T. Uhl, Micromechanical Model for Deformation in Solids with Universal Predictions for Stress-Strain Curves and Slip Avalanches, *Phys. Rev. Lett.* **102**, 175501 (2009).
3. S. Karmakar, E. Lerner, and I. Procaccia, Statistical physics of the yielding transition in amorphous solids, *Phys. Rev. E* **82**, 055103(R) (2010).
4. S. Franz and S. Spigler, Mean-field avalanches in jammed spheres, *Phys. Rev. E* **95**, 022139 (2017).
5. Y. Wang, S. Fang, N. Xu, and Y. Deng, Two-Scale Scenario of Rigidity Percolation of Sticky Particles, *Phys. Rev. Lett.* **124**, 255501 (2020).